A central back-coupling hypothesis on the organization of motor synergies: a physical metaphor and a neural model

M.L. Latash, J.K. Shim, A.V. Smilga, V.M. Zatsiorsky

Published in final edited form as:
Biol Cybern. 2005 March ; 92(3): 186–191. doi:10.1007/s00422-005-0548-0.

A central back-coupling hypothesis on the organization of motor synergies: a physical metaphor and a neural model

Mark L. Latash[1], **Jae Kun Shim**[1], **Andrei V. Smilga**[2], and **Vladimir M. Zatsiorsky**[1]

[1] Department of Kinesiology, Rec.Hall-268N, The Pennsylvania State University, University Park, PA 16802, USA

[2] Department of Theoretical Physics, University of Nantes, Nantes, France

Abstract

We offer a hypothesis on the organization of multi-effector motor synergies and illustrate it with the task of force production with a set of fingers. A physical metaphor, a leaking bucket, is analyzed to demonstrate that an inanimate structure can show apparent error compensation among its elements. A neural model is developed using tunable back-coupling loops as means of assuring error compensation in a task-specific way. The model demonstrates non-trivial features of multi-finger interaction such as delayed emergence of force stabilizing synergies and simultaneous stabilization of the total force and total moment produced by the fingers. The hypothesis suggests that neurophysiological structures involving short-latency feedback may play a central role in the formation of motor synergies.

1 Introduction

Recent studies have addressed the coordinated action of human digits to stabilize such performance variables as the total force and the total moment of forces applied to an external object (Latash et al. 2001, 2002a; Shim et al. 2003, 2004; Zatsiorsky et al. 2003). In those studies, multi-digit synergies were operationally defined as coordinated changes in elemental variables (individual digit forces and moments or hypothetical independent signals to individual digits; reviewed in Latash et al. 2002b; Zatsiorsky and Latash 2004). The studies have shown that individual finger forces/moments co-vary across repetitions of a task to stabilize the resultant force and/or the resultant moment applied either to a fixed external object or to a free hand-held object maintained at rest.

A number of findings have suggested limitations in the ability of the human hand to stabilize the total force applied by a set of digits. In particular, multi-finger pressing tasks have shown preferential stabilization of the pronation/supination moment of forces even when the explicit task and the visual feedback emphasized total force stabilization while no feedback was provided on the moment (Latash et al. 2001, 2002a). In slow ramp force production tasks performed under visual feedback, the initiation of the ramp was always associated with positive covariation of individual finger forces, quantified both across trials and across samples within a single trial, that could stabilize the pronation/supination moment but destabilized the total force (Scholz et al. 2003; Shim et al. 2003). This counter-intuitive relation among finger forces persisted for a certain critical time and was followed by a negative covariation among the finger forces adequate for the total force stabilization. The findings of positive covariation among

Correspondence to: M. L. Latash (mll11@psu.edu, Tel.: +1-814-863-5374).

finger forces early in the trial may be interpreted as pointing at an inability of the controller to organize negative covariation of finger forces – to stabilize the required time profile of the total force – during the initial segment of trial. The critical time was shown to vary between about 100 ms and 800 ms, while during very fast force production trials it dropped to under 40 ms (Latash et al. 2004). Such delays are hardly compatible with an action of proprioceptive feedback loops. Hence, we assume that emergence of negative covariation among finger forces is likely to be based on a central back-coupling mechanism within the central nervous system. We will address this assumption as the central back-coupling (CBC) hypothesis.

2 A rusty bucket metaphor

We would like to illustrate the general idea of the CBC-hypothesis with a simple physical analogy – a rusty bucket metaphor (Fig. 1). Imagine that you have an old bucket with a lot of holes in the bottom. The holes are rusty with uneven edges, with crumbs of metal falling off occasionally. Also, there is rubbish on the bottom of the bucket that sometimes blocks partly some of the holes. Now let us pour water into the bucket at a constant rate. The water will pour out through the holes such that each hole will show a flow related to its time-dependent area, $s_i(t)$, and the level of water accumulated in the bucket, $H(t)$. At some level of water, the pressure will be such that the amounts of water poured into the bucket, $Q(t)$ and out of the holes, $\Sigma q_i(t)$ will be equal, and the system will be in an equilibrium. If we increase the flow of water into the bucket, a new equilibrium will be reached at a new water level corresponding to a higher pressure and proportionally higher outflow. Imagine now that a crumb of metal falls off the edges of one of the holes. It becomes bigger and the amount of water flowing out of the hole increases. As a result, the level of water in the bucket starts to fall down leading to a decrease in the pressure and in the amount of water flowing out of *all the holes*. Ultimately, the water in the bucket will reach a new, lower level corresponding to a new equilibrium.

If one ignores the object in its entirety and looks only at the behavior of its elements (holes), quite an interesting picture emerges: one element (the crumbling hole) introduces a change in its behavior. As a result, all other holes change their behavior (start to let less water through) such that the overall performance variable (the total amount of water flowing out of the bucket) remains unchanged, equal to the amount of water that is being poured in. In more general terms: one element introduced an error into the functioning of the system. Other elements corrected the error (we will call such phenomena error compensation among elements, Gelfand and Latash 1998).

The water balance equation for the rusty bucket is

$$S\frac{\mathrm{d}H}{\mathrm{d}t}=Q-u(H)\sum_{i=1}^{n}s_i(t), \tag{1}$$

where S is the area of the bucket horizontal cross-section, $s_i(t)$ are the fluctuating areas of the individual holes, u is velocity of water outflow from the holes, and n is the total number of holes. For a real rusty bucket, one would have $u=\sqrt{2gH}$, but a mathematical model (and we are obviously interested in the latter rather than in the bucket itself) becomes much simpler if assuming $u \propto H$. To simplify the situation still further, we assume that the area fluctuations are small, $\Delta s_i(t) << s_i(t)$ and their spectrum represents a delta function:

$$\int \mathrm{d}t \left\langle \Delta s_i(t)\,\Delta s_j(0)\right\rangle \mathrm{e}^{iwt} \propto \delta_{ij}\delta(\omega-\omega_0). \tag{2}$$

In other words, the fluctuations are assumed to be periodic,

$$s_i(t) = 1 + \alpha_i \quad \cos(\omega_i t + \varphi_i), \tag{3}$$

with $\alpha << 1$, and $|\omega_i - \omega_j| << \omega_i \approx \tilde{\omega}_0$, but incommensurable frequencies,

$$\langle \cos_i \quad \cos_j \rangle = \langle \sin_i \quad \sin_j \rangle = \frac{1}{2}\delta_{ij}. \tag{4}$$

Getting rid of dimensionful parameters, we can write Eq. (1) in the form:

$$\frac{dH}{dt} + H\left[1 + \frac{\alpha}{n}\sum_{i=1}^{n}\cos(\omega_i t)\right] = 1. \tag{5}$$

This equation can be solved analytically. A general solution to this equation with the initial conditions $H(0) = H_0$ is:

$$\begin{aligned} H(t) = \quad & \exp\left\{-t - \tfrac{\alpha}{n}\sum_i \tfrac{\sin(\omega_i t)}{\omega_i}\right\} \\ & \times\left[H_0 + \int_0^t d\tau \cdot \exp\left\{\tau + \tfrac{\alpha}{n}\sum_i \tfrac{\sin(\omega_i t)}{\omega_i}\right\}\right]. \end{aligned} \tag{6}$$

To illustrate the main features of this model, we will be interested mainly in the long time-scale asymptotics of the solution where all relaxation processes are complete and the result does not depend on initial conditions. Neglecting H_0 in Eq. (6), introducing $y=(t-\tau)$, and extending the integral over dy up to infinity we obtain:

$$\begin{aligned} H(t) \approx \quad & \exp\left\{-\tfrac{\alpha}{n}\sum_i \tfrac{\sin(\omega_i t)}{\omega_i}\right\} \\ & \times\int_0^\infty dy \cdot \exp\left\{\tfrac{\alpha}{n}\sum_i \tfrac{\sin[\omega_i(t-y)]}{\omega_i}\right\}. \end{aligned} \tag{7}$$

Multiplying it by $s_i(t)$ from Eq. (3) gives a quantity proportional to the water flow from the hole i, $q_i = s_i u(H)$. The quantity of interest is the correlation between the flows associated with different holes. When $\alpha << 1$, the correlation coefficients can be easily evaluated by expanding $q_i(t)$ in α up to terms $\propto \alpha^2$ and using the rules (4).

A simple calculation gives the result

$$k_{ij} = -\frac{1}{n - 1 + n\omega_0^2}. \tag{8}$$

The correlation is always negative. In the most simple case of two holes with $\omega_0 << 1$ (physically, $\omega_0 T << 1$, where T is the characteristic relaxation time of the system), the correlation coefficient reaches its maximal absolute value, $k = -1$.

A measure of finger force covariation (ΔV) was introduced in earlier studies (Scholz et al. 2003; Shim et al. 2004):

$$\Delta V(t) = \frac{\sum_{j=1}^{n} \mathrm{Var}_{F_j}(t) - \mathrm{Var}_{F_{\mathrm{TOT}}}(t)}{\sum_{j=1}^{n} \mathrm{Var}_{F_j}(t)}, \tag{9}$$

where Var_{Fj} stands for the variance of the force produced by finger j [j = index(i), middle (m), ring (r), and little (l) fingers] and $\mathrm{Var}_{F\mathrm{TOT}}$ stands for the variance of the total force produced by all fingers. Note that both Var indices were computed over a set of trials at a multi-finger task at each moment of time, such that ΔV in this expression is a time function. An analogous steady-state index can be computed for the outflows of water from different holes in our model. We obtain:

$$\begin{aligned} \Delta V &= \frac{2\sum_{i<j}\left[\langle q_i\rangle\langle q_j\rangle - \langle q_i q_j\rangle\right]}{\sum_{i}\left[\langle q_i^2\rangle - \langle q_i\rangle^2\right]} \\ &= -(n-1)\,k_{ij} = \frac{1}{1+\frac{n}{n-1}\omega_0^2}. \end{aligned} \tag{10}$$

A few conclusions can be made. First, the index ΔV is always positive meaning a negative covariation among water outflows from the holes. Second, an increase in the number of holes over two leads to relatively small changes (a mild increase) in ΔV . Third, there is a strong dependence of ΔV and pair correlations k_{ij} on ω_0: When the frequency is high as compared to the inverse characteristic relaxation time of the system, the level of water H cannot follow the fluctuations of $s_i(t)$ and the correlations disappear. The rusty bucket functions on the principle of conservation of matter. The neural network needs to have explicit feedbacks to emulate such a mechanism. Besides, we would like the neural network to be able to change its functioning in a task-specific manner. This leads us to the following hypothesis.

The controller creates synergies by adjusting gains at central feedback loops among neuronal structures (“neurons”) whose output specifies values of elemental variables. Emergence of a synergy among the elemental variables may be associated with creation of a gain matrix [**G**] – partly analogous to the control matrices introduced by Gelfand and Tsetlin (1966), which links outputs from a set of neurons to feedback inputs to the same neurons.

We are going to illustrate this hypothesis with an example of control of four fingers of the human hand involved in tasks that require the production of an accurate time profile of force and/or of a constant moment with respect to the longitudinal axis of the hand/forearm (pronation/supination moment). Since we are interested in the patterns of finger force covariation, we did not introduce in this model the phenomenon of force deficit, which, for a given number of fingers, would simply result in scaling of the outputs of all fingers with a constant coefficient (Danion et al. 2003).

3 The central back-coupling model

The CBC-model (Fig. 2) uses a plausible neural mechanism of self- and lateral inhibition among the elements (output neurons). Such connections were described for various neurophysiological structures (e.g., the well-known system of Renshaw cells, Rothwell 1994) and were also used in “winner-takes-all” artificial neural nets (Kincaid et al. 1996;Lund et al. 2003). In Fig. 2, a command signal (level A) is being distributed over four neurons producing a particular sharing pattern, $\mathbf{S(t)} = [s_i, s_m, s_r, s_l]$, where the subscripts refer to individual fingers. We accepted a sharing pattern of [0.31, 0.29, 0.21, 0.19] as a typical pattern

seen during four-finger force production tasks in young healthy subjects (Li et al. 1998;Zatsiorsky et al. 1998,2000). This signal is assumed to be noisy (Gaussian noise with zero average is added) leading to inputs to individual neurons (level B) that deviate randomly from those prescribed by the sharing, $\mathbf{S_B(t)} = \mathbf{S(t)} + \mathbf{N(t)}$, where $\mathbf{N} = [n_i, n_m, n_r, n_l]$ is a noise vector. The output of each of the level B neurons serves as the input to an interneuron (four INs at level C), which projects back to all four level B neurons. These back-coupling loops are characterized by gains (g_{ij} comprising a matrix **G**), time delays (Δt), and thresholds (Thr). Hence, the total input to the level B neurons, $\mathbf{B_{IN}}(t) = \mathbf{S_B}(t) + [\mathbf{G}]\mathbf{m}(t - \Delta t)$, where $\mathbf{m}(t)$ is the output of level B neurons. Besides projecting on level C interneurons, this output is also transformed by a finger interconnection matrix [**E**], also addressed as an enslaving matrix (Zatsiorsky et al. 1998) resulting in finger forces: $\mathbf{f} = [\mathbf{E}]\mathbf{m}$.

Our preliminary analysis was limited to a case of all $g_{ij} < 0$, $\Delta t = 10$ ms, Thr = 0.05 N, and a task of ramp force production from zero to 30 N over 3 s (for simplicity, all signals in the network are expressed in newtons). **G** may be viewed as a synergy matrix that defines patterns of covariation among the outputs of the elements. The **E** matrix was taken to represent typical values (Zatsiorsky et al. 2000) with an average enslaving of about 10% of corresponding MVC forces. The noise level was set proportional to the sharing with the average standard deviation of 0.05.

4 Network testing

Figure 3a illustrates the time profiles of individual finger forces for a typical trial at the task by the described neural network. In this example, all g_{ij} were set at –0.33. The sharing pattern was selected to reflect actually observed typical sharing patterns during such tasks (Latash et al. 2002a; Shim et al. 2003). The network performed the task 12 times. Time profiles of the sum of the variances of the individual finger forces [$\Sigma \mathrm{Var}_{Fi}(t)$] and the variance of the total force [$\mathrm{Var}_{FTOT}(t)$] were computed over the twelve trials; the difference between the two was also computed and divided by $\Sigma \mathrm{Var}_{Fi}(t)$ [$\Delta V_F(t)$]. Figure 3b illustrates a typical time profile of $\Delta V_F(t)$. Note that $\Delta V_F(t)$ is negative early in the trial corresponding to positive covariation among the finger forces. After about 200–300 ms, $\Delta V_F(t)$ turns and remains positive corresponding to negative covariation of the finger forces, i.e. total force stabilization. Such transients were not analyzed in the rusty bucket metaphor. In that model, all processes are assumed to be ruled by the laws of physics (hydrostatics) without time delays. Hence, no special behavior is expected early in the transition period.

Using the same data, we also computed variance time profiles of the moments of forces produced by the fingers with respect to the midpoint between the middle and ring fingers. We assumed that the fingers are aligned along a straight line at 3 cm intervals, a typical configuration in many earlier studies (Li et al. 1998; Latash et al. 2001, 2002a; Shim et al. 2003). Hence, the lever arm magnitudes for the two lateral fingers were assumed 4.5 cm, while the lever arms for the two central fingers were assumed 1.5 cm. The dashed line in Fig. 3b illustrates $\Delta V_M(t)$ computed similarly to the force variance profiles but taking into account the different lever arms of individual fingers (including the difference in their signs). Note that $\Delta V_M(t)$ is negative over most of the trial duration.

Further, we have explored the importance of the g_{ij} entries of the synergy matrix [**G**]. Figure 4 illustrates what happens with $\Delta V_F(t)$ and $\Delta V_M(t)$ time profiles when two of the g_{ij} entries are set to positive numbers ($g_{il} = g_{li} = 0.15$, where i and l stand for the index and little fingers, respectively). This figure shows that the neural net can generate patterns of finger force covariation that stabilize both the total force and the total moment corresponding to experimental observations (Shim et al. 2003;Shinohara et al. 2003).

To provide another link to the "rusty bucket" model, we have analyzed the effects of changing the mean power frequency of the noise signal, $\mathbf{N}(t)$ on ΔV. According to Eq. (10), an increase in the frequency of the signal (ω_0) should lead to a drop in ΔV. Figure 5 illustrates the dependence of ΔV on the mean power frequency of the noise signal for the neural model; ΔV was computed over twelve realizations of the task, for each moment of time, and then averaged over the task duration. The figure shows a close to linear drop in ΔV with an increase in the mean power frequency of $\mathbf{N}(t)$.

5 Discussion

Our study has shown that certain salient features of multi-finger synergies, such as error compensation, may result from a central back-coupling mechanism. As such, they do not necessarily require action of proprioceptive feedback loops (cf. Todorov and Jordan 2002). This does not mean, of course, that a similar error correction mechanism cannot make use of the proprioceptive information. Rather, that the relative role of this information inflow may vary. The suggested scheme was able to reproduce some of the less trivial results of recent studies, including a switch from positive to negative covariation among finger forces at a certain critical time (Shim et al. 2003). It has also been able to demonstrate both total force and total moment stabilization simultaneously as well as preferential total moment stabilization early in the task, even though the task input specified a time profile of the total force but not of the total moment (Latash et al. 2001, 2002b).

Short-latency negative feedback loops, also addressed as lateral inhibition and surround suppression, are rather common in the central nervous system. They have been described and/or postulated for sensory system of different modalities (Lund et al. 2003; Schoppa and Urban 2003; Wehr and Zador 2003; Ozeki et al. 2004) as well as for brain circuits traditionally associated with the production of movement (Fukai 1999).

Typically, the function of lateral inhibition was discussed as related to detecting small changes in the magnitude of a signal (Litvinov 2002; Urban 2002) or optimizing temporal precision in signal detection (Wehr and Zador 2003). As our model suggests, such feedback loops may play a more subtle role in the control of the output of neuronal pools, in particular stabilizing the level of the output or its particular functional form, e.g. the total moment produced by the fingers in the model. Changing the strength of the feedback projections in such systems may be viewed as a means of adjusting the functioning of the pool in a task-specific way (e.g., Guzman et al. 2003).

The well-known system of Renshaw cells (recurrent inhibition) has recently become incorporated into several hypotheses on the control of movement (van Heijst et al. 1998; Uchiyama et al. 2003). There is substantial variability in the organization and the strength of inhibitory projections mediated by Renshaw cells in different muscles (Katz et al. 1993). These projections can be modulated pharmacologically and by descending projections (Mattei et al. 2003; Hultborn et al. 2004). According to the current model, such organization favors a role of the Renshaw cells in stabilizing the output of a motoneuronal pool in a way that could be muscle- and task-specific (cf. Hultborn et al. 2004). Certainly, our analysis does not imply that projections of Renshaw cells on motoneurons can change from inhibitory to excitatory. However, modulation of the strength of inhibitory projections may be expected to change the degree of stabilization of the total output of the motoneuronal pool. Similarly designed systems with short-latency back-coupling projections that can change both gain and sign of their action may be expected to be more powerful in their ability to stabilize different output functions.

In earlier publications (Gelfand and Latash 1998; Latash et al. 1998), we suggested that motor synergies were defined by two features, sharing (e.g., Li et al. 1998; Tresch et al. 1999; Saltiel

et al. 2001; Ivanenko et al. 2004) and error compensation (e.g., Abbs and Gracco 1984; Kelso et al. 1984; Berkinblit et al. 1986; Latash et al. 1998), and claimed that error compensation was a more salient feature because stable sharing among a few components is typical of many inanimate objects such as the prongs of a fork or the legs of a table. We have apparently underestimated the sophistication of the inanimate nature. The rusty bucket example shows that a rather mundane object can demonstrate features that look like error compensation. There is one feature of the CBC-model, however, that no inanimate object seems to be able to replicate, that is, its ability to change the covariation pattern of the elements (with the help of the **G** matrix) in a task-specific manner.

We see the notion of a **G** matrix as central to the hypothesis. Adjustments in **G** may occur independently of the task (Fig. 2). As such, this scheme allows for changes in patterns of covariation among elemental variables without a change in their combined output. Our recent experiments have shown that, indeed, the index of finger force covariation (ΔV) shows changes about 100 ms prior to a change in the total force when the task requires a quick change in the total force (Shim et al. 2005). We have termed this phenomenon “anticipatory covariation”; the CBC-model provides a scheme that can account for anticipatory covariation in the absence of visible changes in the combined output of the system.

References

Abbs JH, Gracco VL. Control of complex motor gestures: Orofacial muscle responses to load perturbations of the lip during speech. J Neurophysiol 1984;51:705–723. [PubMed: 6716120]

Berkinblit MB, Feldman AG, Fukson OI. Adaptability of innate motor patterns and motor control mechanisms. Behav Brain Sci 1986;9:585–638.

Danion F, Schöner G, Latash ML, Li S, Scholz JP, Zatsiorsky VM. A force mode hypothesis for finger interaction during multi-finger force production tasks. Biol Cybern 2003;88:91–98. [PubMed: 12567224]

Fukai T. Sequence generation in arbitrary temporal patterns from theta-nested gamma oscillations: a model of the basal ganglia-thalamo-cortical loops. Neural Netw 1999;12:975–987. [PubMed: 12662640]

Gelfand IM, Latash ML. On the problem of adequate language in motor control. Motor Control 1998;2:306–313. [PubMed: 9758883]

Gelfand, IM.; Tsetlin, ML. On mathematical modeling of the mechanisms of the central nervous system.. In: Gelfand, IM.; Gurfinkel, VS.; Fomin, SV.; Tsetlin, ML., editors. Models of the structural-functional organization of certain biological systems. Nauka; Moscow: 1966. p. 9-26.(in Russian, a translation is available in 1971 edition by MIT Press, Cambridge)

Guzman JN, Hernandez A, Galarraga E, Tapia D, Laville A, Vergara R, Aceves J, Bargas J. Dopaminergic modulation of axon collaterals interconnecting spiny neurons of the rat striatum. J Neurosci 2003;23:8931–8940. [PubMed: 14523095]

Hultborn H, Brownstone RB, Toth TI, Gossard JP. Key mechanisms for setting the input-output gain across the motoneuron pool. Prog Brain Res 2004;143:77–95. [PubMed: 14653153]

Ivanenko YP, Poppele RE, Lacquaniti F. Five basic muscle activation patterns account for muscle activity during human locomotion. J Physiol 2004;556:267–282. [PubMed: 14724214]

Katz R, Mazzocchio R, Penicaud A, Rossi A. Distribution of recurrent inhibition in the human upper limb. Acta Physiol Scand 1993;149:183–198. [PubMed: 8266808]

Kelso JA, Tuller B, Vatikiotis-Bateson E, Fowler CA. Functionally specific articulatory cooperation following jaw perturbations during speech: evidence for coordinative structures. J Exp Psychol: Hum Percept Perform 1984;10:812–832. [PubMed: 6239907]

Kincaid TG, Cohen MA, Fang Y. Dynamics of a winner-take-all neural network. Neural Netw 1996;9:1141–1154. [PubMed: 12662589]

Latash ML, Li ZM, Zatsiorsky VM. A principle of error compensation studied within a task of force production by a redundant set of fingers. Exp Brain Res 1998;122:131–138. [PubMed: 9776511]

Latash ML, Scholz JF, Danion F, Schöner G. Structure of motor variability in marginally redundant multi-finger force production tasks. Exp Brain Res 2001;141:153–165. [PubMed: 11713627]

Latash ML, Scholz JF, Danion F, Schöner G. Finger coordination during discrete and oscillatory force production tasks. Exp Brain Res 2002a;146:412–432.

Latash ML, Scholz JP, Schöner G. Motor control strategies revealed in the structure of motor variability. Exer Sport Sci Rev 2002b;30:26–31.

Latash ML, Shim JK, Zatsiorsky VM. Is there a timing synergy during multi-finger production of quick force pulses? Exp Brain Res 2004;159:65–71. [PubMed: 15480588]

Li ZM, Latash ML, Zatsiorsky VM. Force sharing among fingers as a model of the redundancy problem. Exp Brain Res 1998;119:276–286. [PubMed: 9551828]

Litvinov EG. Lateral inhibition as a possible mechanism for evaluating stimulus intensity. Neurosci Behav Physiol 2002;32:231–235. [PubMed: 12135334]

Lund JS, Angelucci A, Bressloff PC. Anatomical substrates for functional columns in macaque monkey primary visual cortex. Cereb Cortex 2003;13:15–24. [PubMed: 12466211]

Mattei B, Schmied A, Mazzocchio R, Decchi B, Rossi A, Vedel JP. Pharmacologically induced enhancement of recurrent inhibition in humans: effects on motoneurone discharge patterns. J Physiol 2003;548:615–629. [PubMed: 12611926]

Ozeki H, Sadakane O, Akasaki T, Naito T, Shimegi S, Sato H. Relationship between excitation and inhibition underlying size tuning and contextual response modulation in the cat primary visual cortex. J Neurosci 2004;24:1428–1438. [PubMed: 14960615]

Rothwell, JC. Control of human voluntary movement. 2nd edn.. Chapman and Hill; London: 1994.

Saltiel P, Wyler-Duda K, D'Avella A, Tresch MC, Bizzi E. Muscle synergies encoded within the spinal cord: evidence from focal intraspinal NMDA iontophoresis in the frog. J Neurophysiol 2001;85:605–619. [PubMed: 11160497]

Scholz JP, Kang N, Patterson D, Latash ML. Uncontrolled manifold analysis of single trials during multi-finger force production by persons with and without Down syndrome. Exp Brain Res 2003;153:45–58. [PubMed: 12928761]

Schoppa NE, Urban NN. Dendritic processing within olfactory bulb circuits. Trends Neurosci 2003;26:501–506. [PubMed: 12948662]

Shim JK, Lay B, Zatsiorsky VM, Latash ML. Age-related changes in finger coordination in static prehension tasks. J Appl Physiol 2004;97:213–224. [PubMed: 15003998]

Shim JK, Latash ML, Zatsiorsky VM. The central nervous system needs time to organize task-specific covariation of finger forces. Neurosci Lett 2003;353:72–74. [PubMed: 14642441]

Shim JK, Olafsdottir H, Zatsiorsky VM, Latash ML. The emergence and disappearance of multi-digit synergies during force production tasks. Exp Brain Res. 2005 in press.

Shinohara M, Latash ML, Zatsiorsky VM. Age effects on force production by the intrinsic and extrinsic hand muscles and finger interaction during maximal contraction tasks. J Appl Physiol 2003;95:1361–1369. [PubMed: 12626484]

Todorov E, Jordan MI. Optimal feedback control as a theory of motor coordination. Nay Neurosci 2002;5:1226–1235.

Tresch MC, Saltiel P, Bizzi E. The construction of movement by the spinal cord. Nat. Neurosci 1999;2:162–167. [PubMed: 10195201]

Uchiyama T, Johansson H, Windhorst U. Static and dynamic input-output relations of the feline medial gastrocnemius motoneuron-muscle system subjected to recurrent inhibition: a model study. Biol Cybern 2003;89:264–273. [PubMed: 14605891]

Urban NN. Lateral inhibition in the olfactory bulb and in olfaction. Physiol Behav 2002;77:607–612. [PubMed: 12527007]

van Heijst JJ, Vos JE, Bullock D. Development in a biologically inspired spinal neural network for movement control. Neural Netw 1998;11:1305–1316. [PubMed: 12662751]

Wehr M, Zador AM. Balanced inhibition underlies tuning and sharpens spike timing in auditory cortex. Nature 2003;426:442–446. [PubMed: 14647382]

Zatsiorsky VM, Gao F, Latash ML. Prehension synergies: effects of object geometry and prescribed torques. Exp Brain Res 2003;148:77–87. [PubMed: 12478398]

Zatsiorsky VM, Latash ML. Prehension synergies. Exer Sport Sci Rev 2004;32:75–80.

Zatsiorsky VM, Li Z-M, Latash ML. Coordinated force production in multi-finger tasks. Finger interaction and neural network modeling. Biol Cybern 1998;79:139–150. [PubMed: 9791934]

Zatsiorsky VM, Li Z-M, Latash ML. Enslaving effects in multi-finger force production. Exp Brain Res 2000;131:187–195. [PubMed: 10766271]

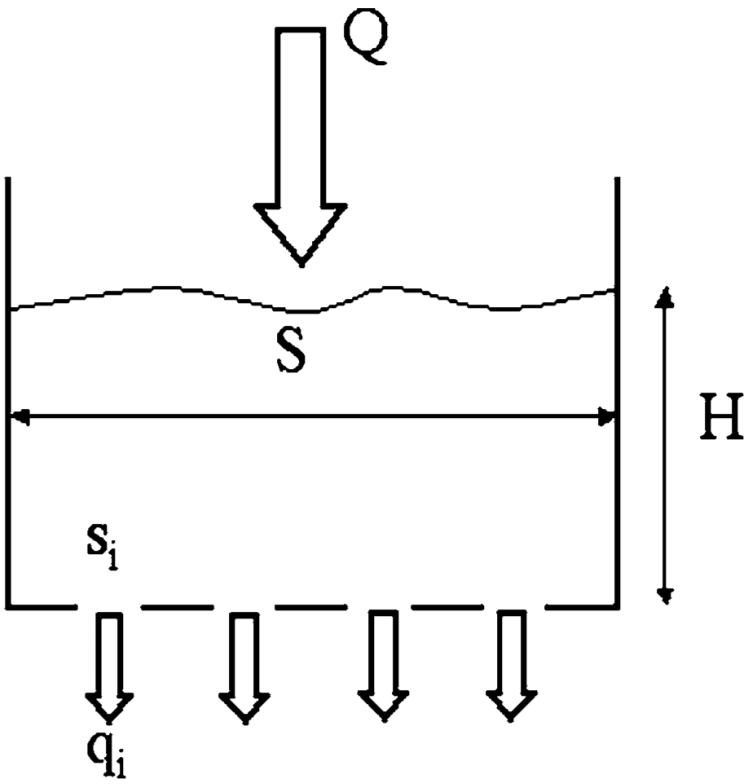

Fig. 1.
The rusty bucket metaphor. Water is poured at a rate Q into the bucket with the total cross-sectional area S. The holes in the bottom have areas s_i and water outflow q_i that depends on the water level H

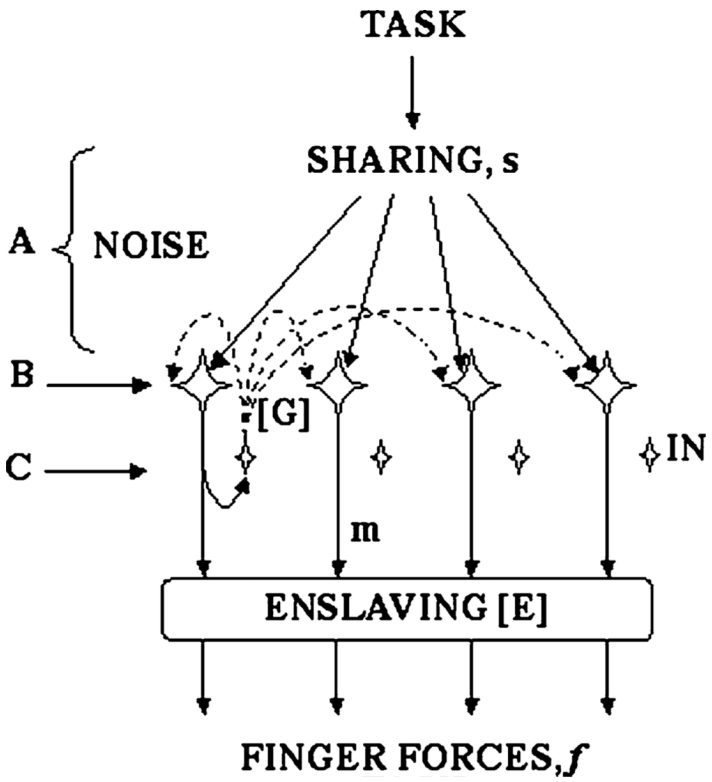

Fig. 2.

The network forming the basis for the CBC-model. At level A, the task is shared among four elements resulting in a vector **s** with added noise. Outputs of neurons at level B, **m** project on INs at level C and also are transformed by an enslaving matrix [**E**]toformforces **f**. All INs at level C project on all neurons at level B; these effects are described with a matrix [**G**]. *Dashed lines* with arrows show inhibitory projections

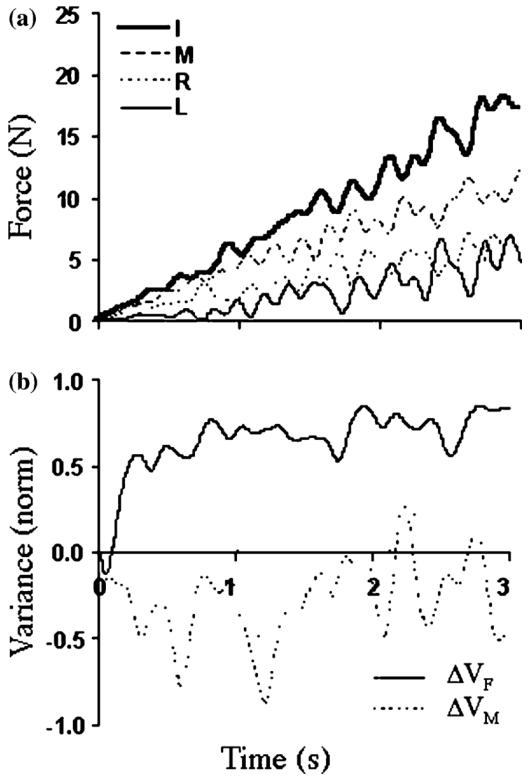

Fig. 3.

a Time profiles of individual finger forces for a representative trial generated by the network shown in Fig. 2. **b** ΔV_F (*solid line*) and ΔV_M (*dotted line*) indices computed over a series of 12 trials at the same task. Note that ΔV_F starts with negative values and turns positive after about 200 ms. ΔV_M stays mostly negative over the duration of the task

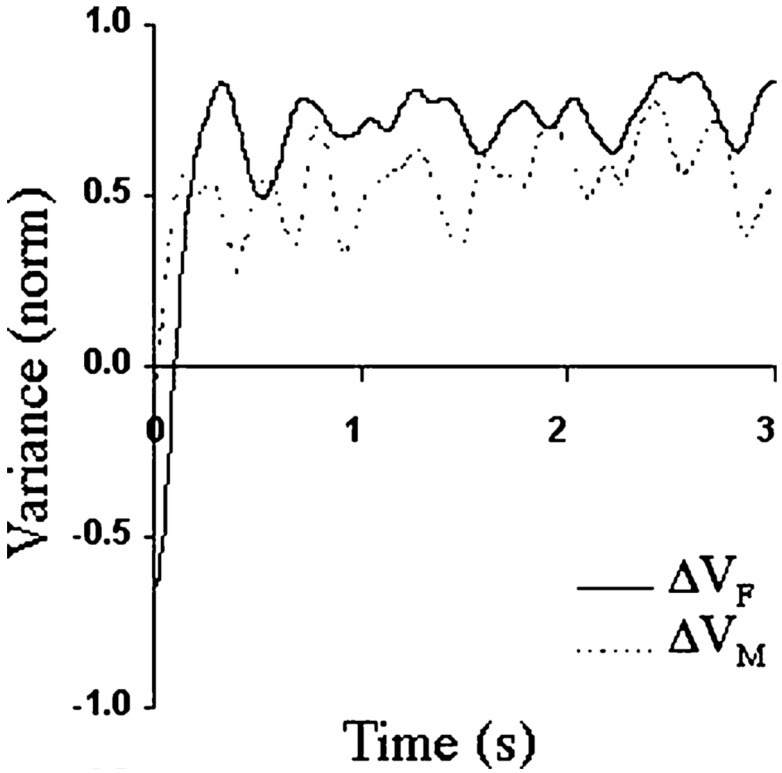

Fig. 4.

ΔV_F (*solid line*) and ΔV_M (*dotted line*) indices computed over a series of twelve trials at the task of producing a ramp profile of the total force. Two indices in the **G** matrix were set positive. Note that ΔV_F starts with negative values and turns positive after about 200 ms. ΔV_M stays positive over the duration of the task

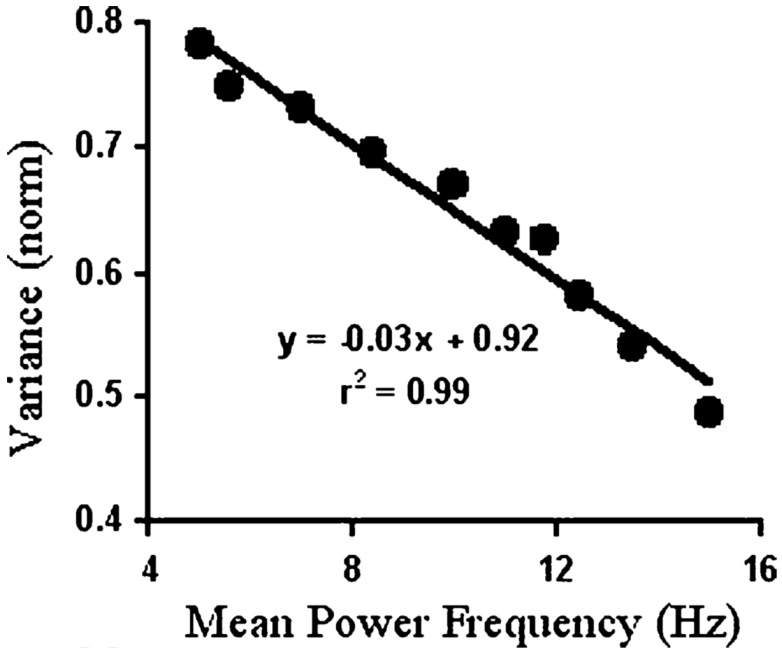

Fig. 5.

The dependence of ΔV on the mean power spectrum frequency of the noise signal. The index ΔV for total force stabilization was computed over 12 realizations of the task for each moment of time. It was further averaged across all time samples. Note that ΔV drops with an increase in the noise mean power spectrum frequency as predicted by Eq. (10). A linear regression line and equation are presented